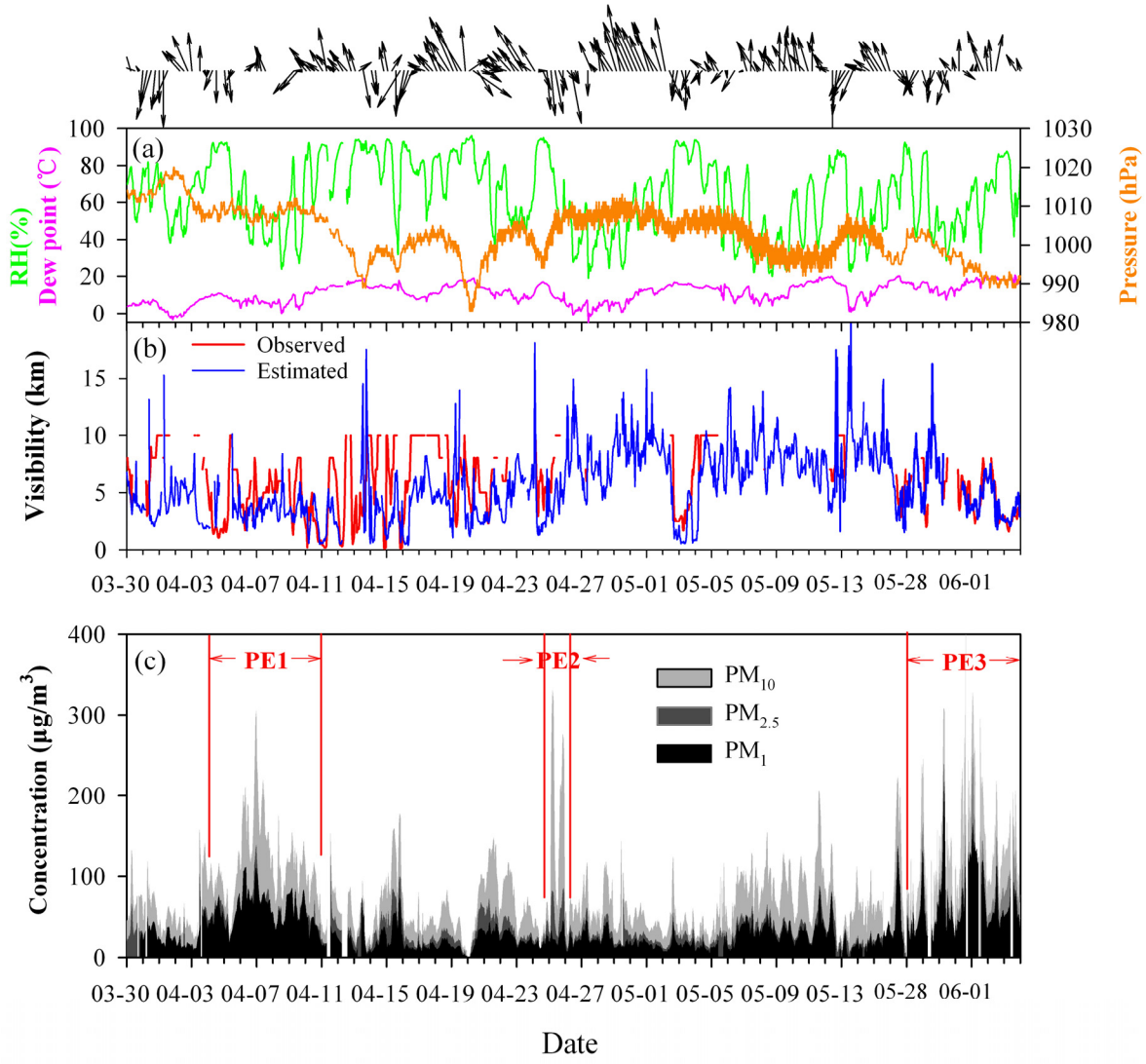

Fig. 1. (a) Time-series of the meteorological parameters during the study period (30 March ~ 16 May and 28 May ~ 3 June) in 2009 over Shanghai, including wind speed (ms^{-1}), wind direction, relatively humidity (%), dew point (℃) and atmospheric pressure (hPa) (b) Time-series of the calculated and observed hourly visibility (km) during the same study period as above. The observed visibility recorded at Pudong had an upper limit of 10km (Data source: National Climatic Data Center (NCDC)). The method of calculating the visibility was described in Appendix A. (b) Time-series of the hourly particulate concentrations of PM_1, $PM_{2.5}$ and PM_{10} (μgm^{-3}), three pollution episodes were highlighted in the figure.

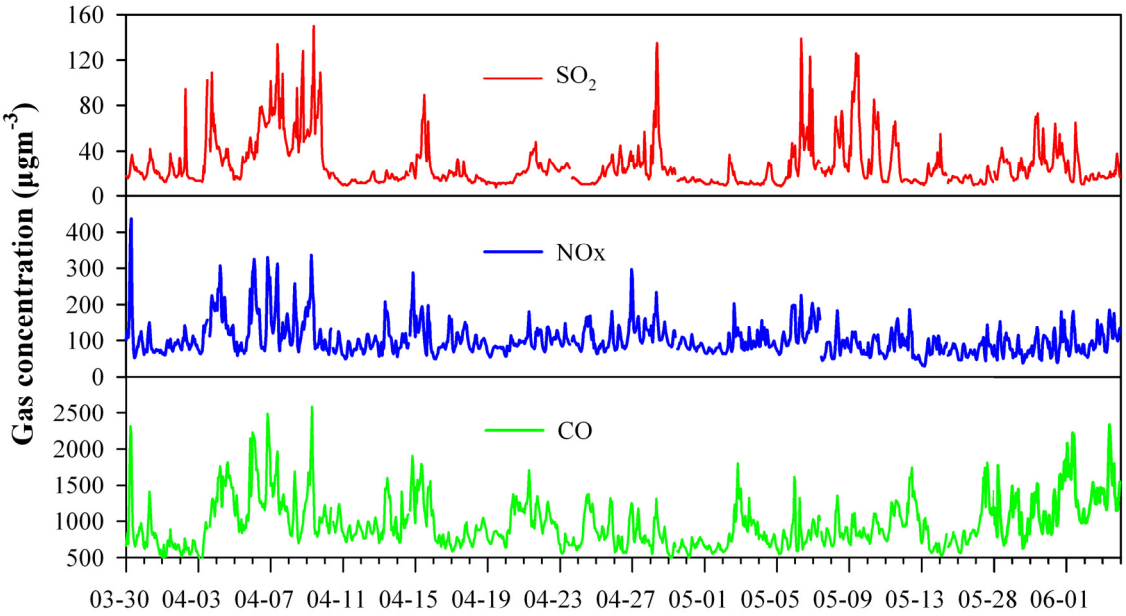

Fig. 2. Time-series of the hourly gaseous concentrations of SO_2, NOx and CO, all units are in μgm^{-3}.

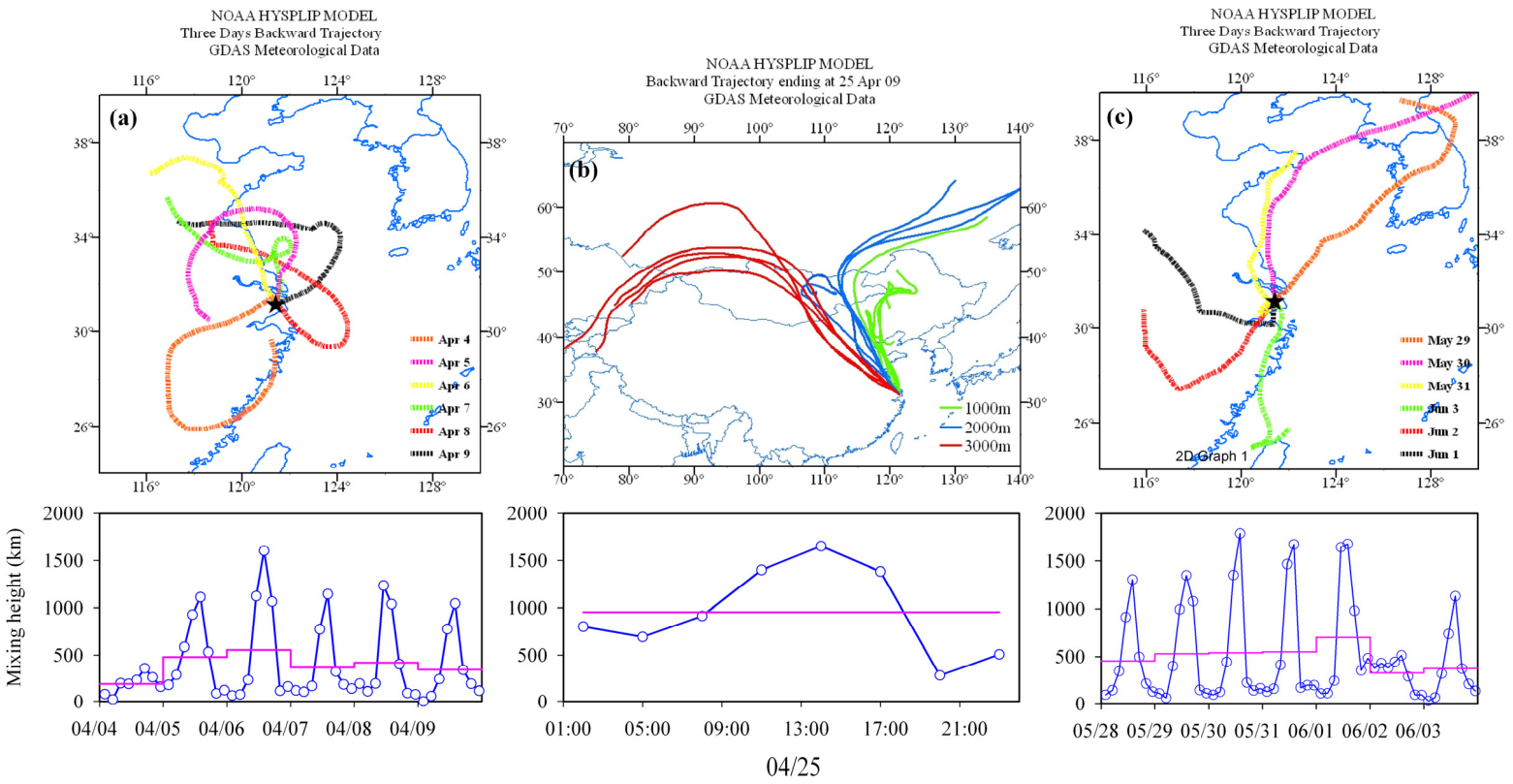

Fig. 3. Three days air mass backward trajectory at Shanghai computed by the NOAA Hybrid Single-Particle Lagrangian Trajectory (HYSPLIT) model during (a) PE1, (b) PE2, and (c) PE3, respectively. The starting altitude during PE1 and PE3 was 500m and three altitudes of 500, 1000 and 1500m were computed during PE2. The mixing heights during three episodes were were computed from the NCEP Global Data Assimilation System (GDAS) model (http://ready.arl.noaa.gov/READYamet.php) and shown below the trajectory panel (blue dots denoted the 3-hr average mixing height and the pink horizontal step lines denoted the daily average mixing height).

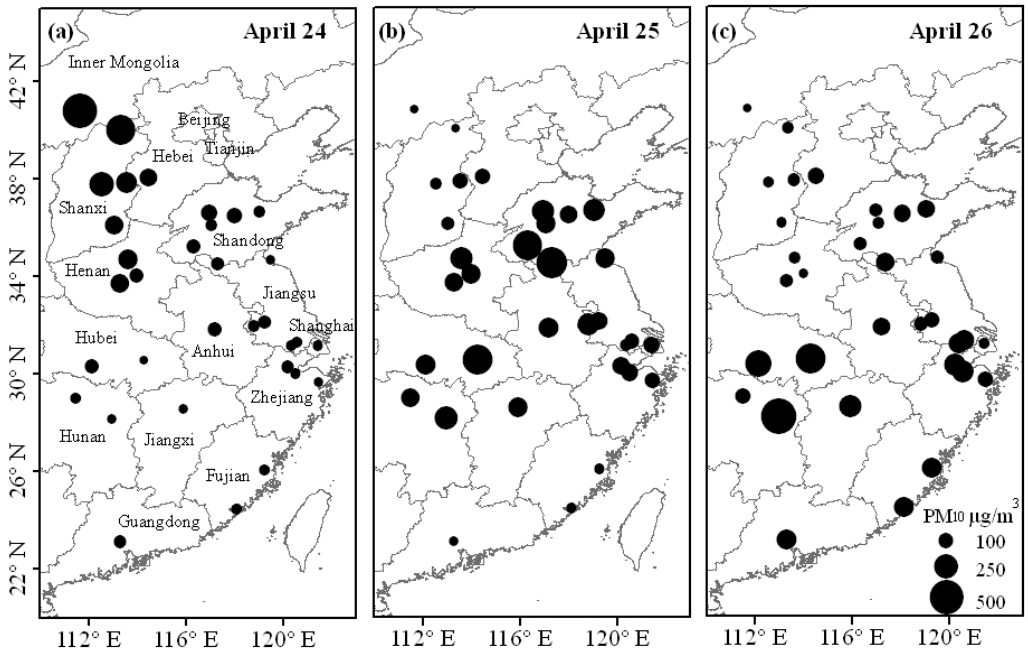

Fig. 4. Regional distribution of PM_{10} concentration (μgm^{-3}) during 24-26 April (Data source: Ministry of Environment Protection of the PRC, http://www.zhb.gov.cn/).

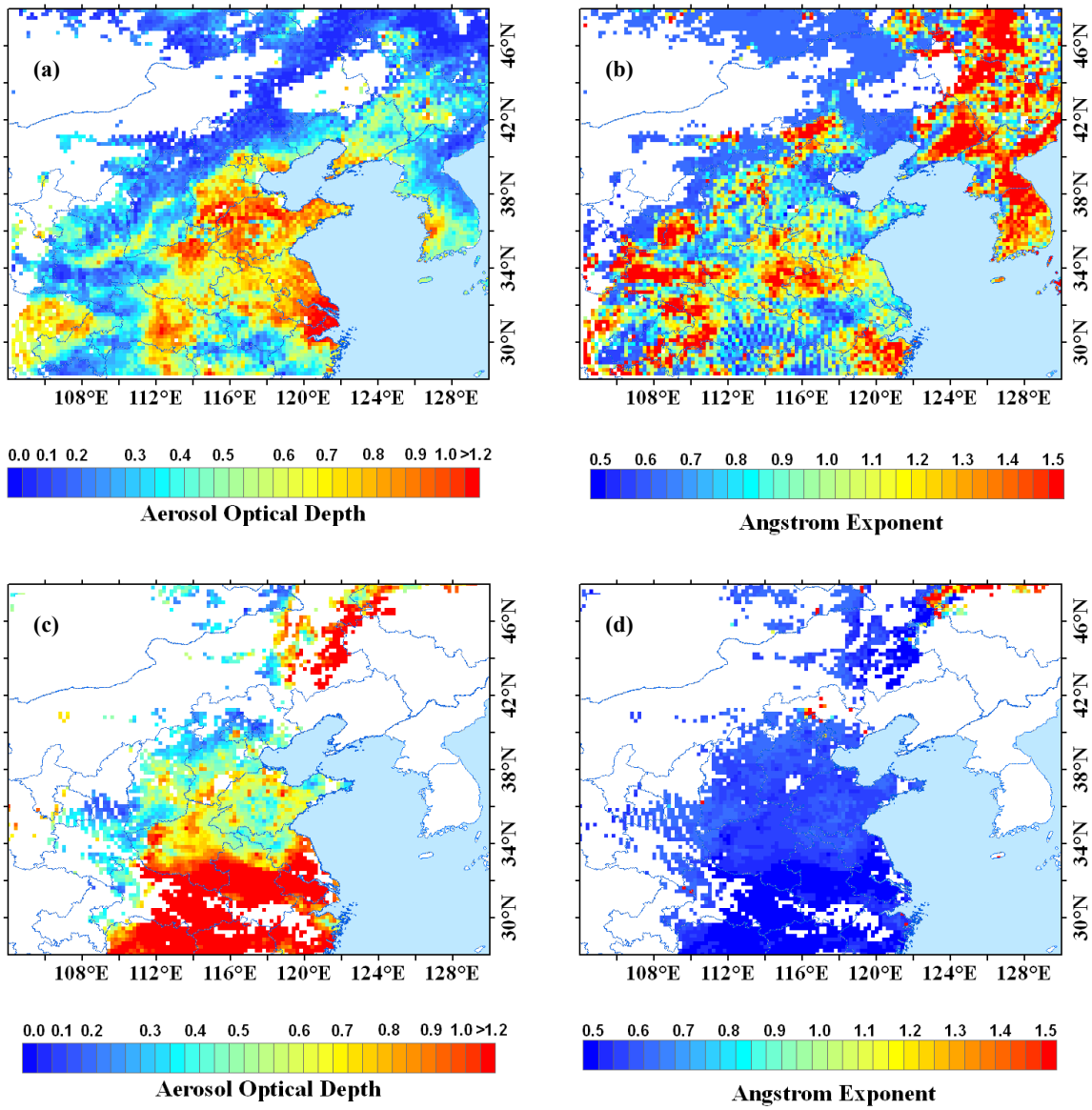
(a)
(b)
(c)
(d)
46°N
42°N
38°N
34°N
30°N
108°E
112°E
116°E
120°E
124°E
128°E
0.0 0.1 0.2 0.3 0.4 0.5 0.6 0.7 0.8 0.9 1.0 >1.2
Aerosol Optical Depth
0.5 0.6 0.7 0.8 0.9 1.0 1.1 1.2 1.3 1.4 1.5
Angstrom Exponent

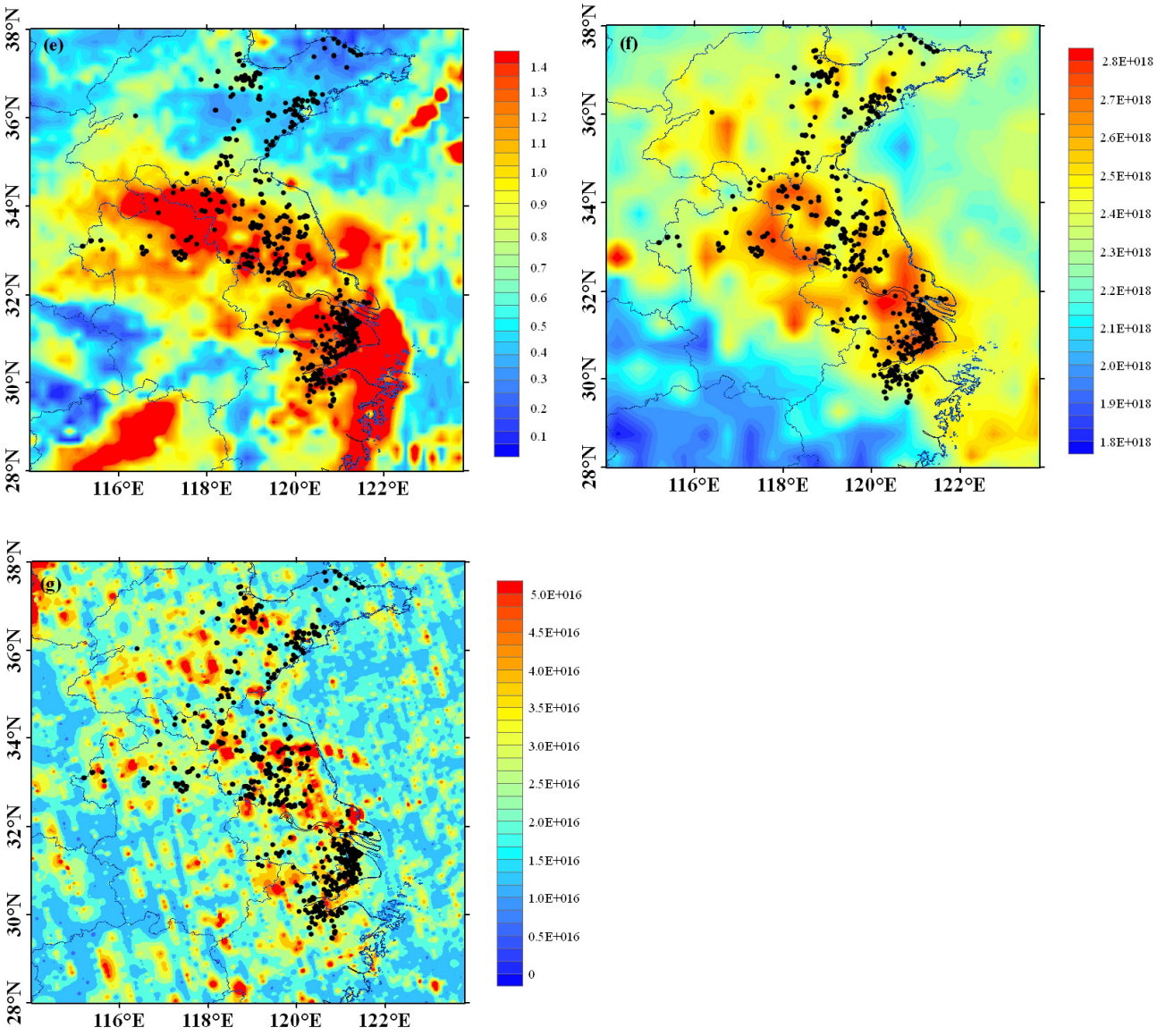

Fig. 5. The regional distribution of (a) aerosol optical depth (550 nm), and (b) Ångström exponent (470 – 670 nm) retrieved from MODIS during PE1; (c) aerosol optical depth, and (d) Ångström exponent during PE2; (e) aerosol optical depth, (f) total CO column concentration (molecules cm^{-2}) retrieved from AIRS, and (g) total formaldehyde column concentration (molecules cm^{-2}) retrieved from OMI during PE3, respectively. Total fire spots (black dots in the figure) retrieved from MODIS were plotted during PE3.

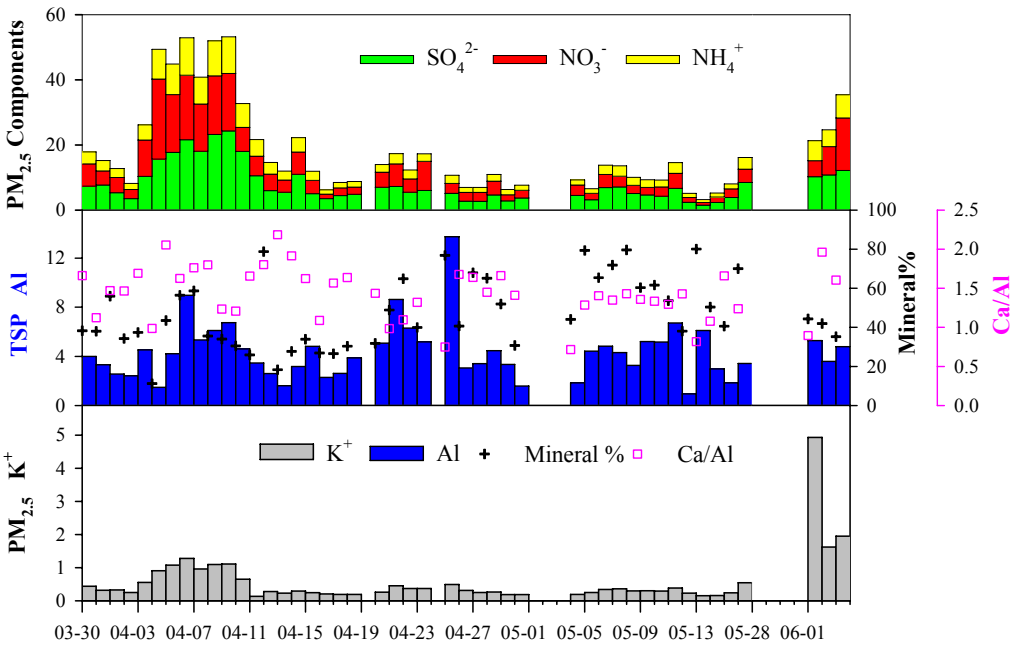

Fig. 6. Time series of (a) SO_4^{2-}, NO_3^-, and NH_4^+ concentration (μgm^{-3}) in $PM_{2.5}$ (b) Al concentration (μgm^{-3}), the fraction of mineral aerosol, and the elemental ratio of Ca/Al in the total suspended particles (TSP) (c) K^+ in $PM_{2.5}$, during the whole study period (Missing data were due to rainfall or malfunction of instruments).

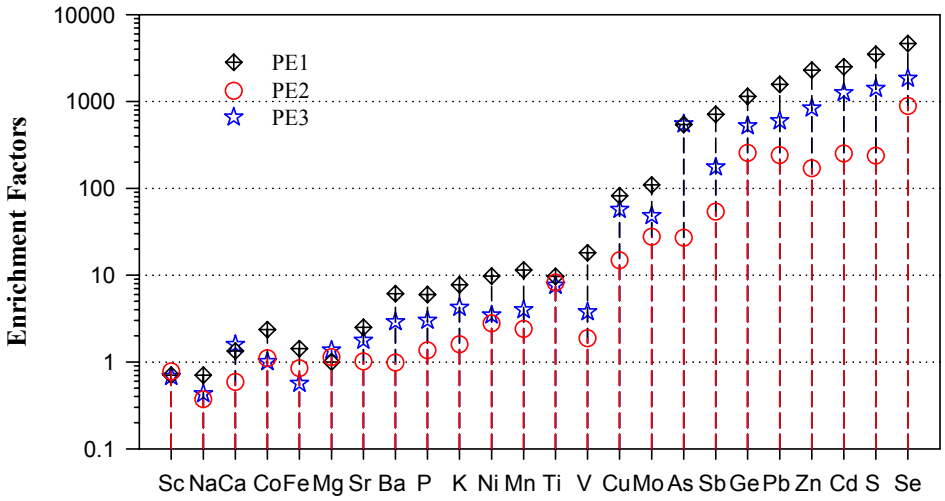

Fig. 7. The average enrichment factors (EF) of various elements during PE1, PE2, and PE3, respectively.

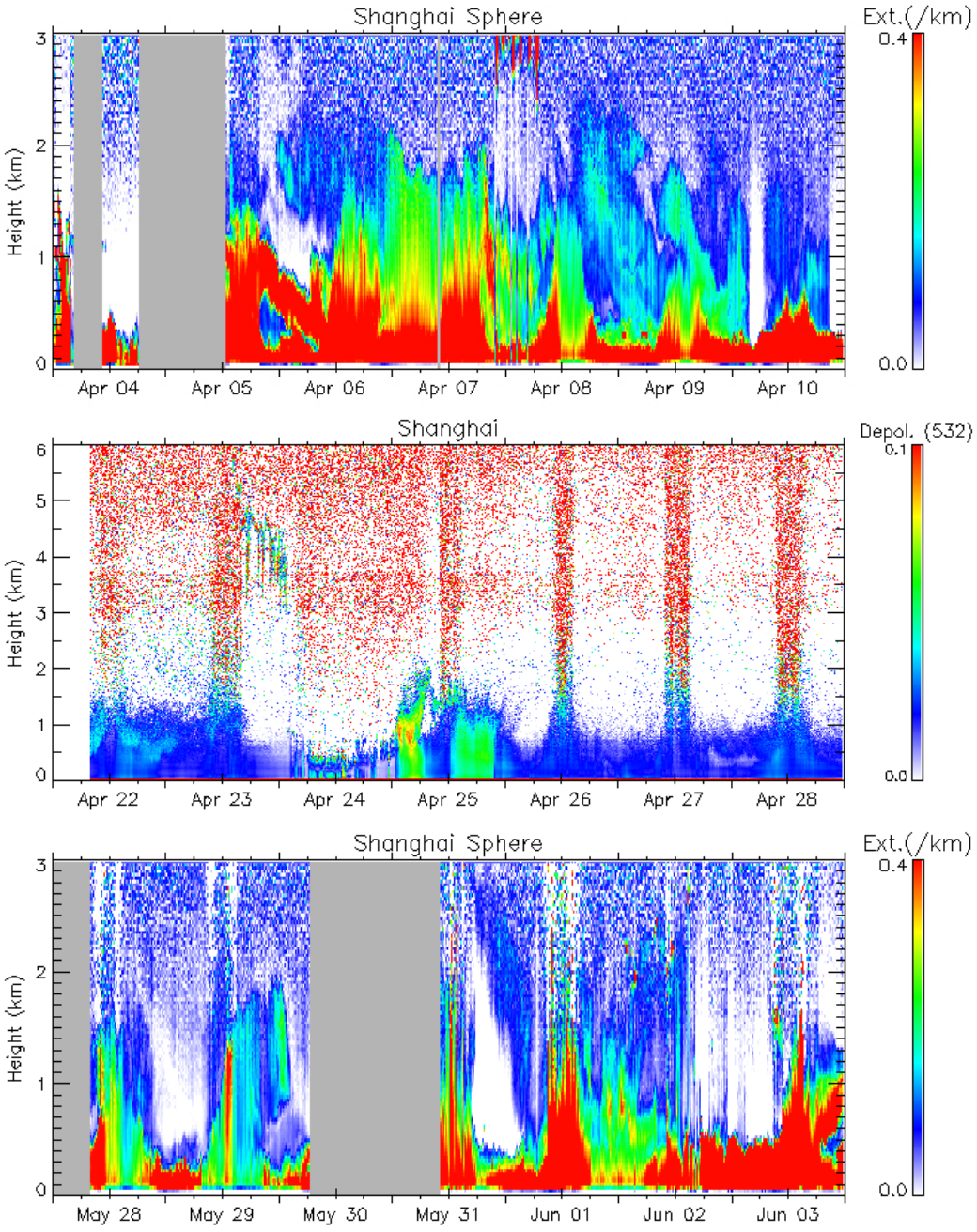

Fig. 8. Top panel: The time-height cross section of spheric aerosol extinction coefficient (km^{-1}) during PE1. Middle panel: The time-height cross section of depolarization ratio from 22-28, April, including PE2 (25 April). Bottom panel: The time-height cross section of spheric aerosol extinction coefficient (km^{-1}) during PE3. The gray columns represented the missing data which were due to the malfunction of the lidar instrument.

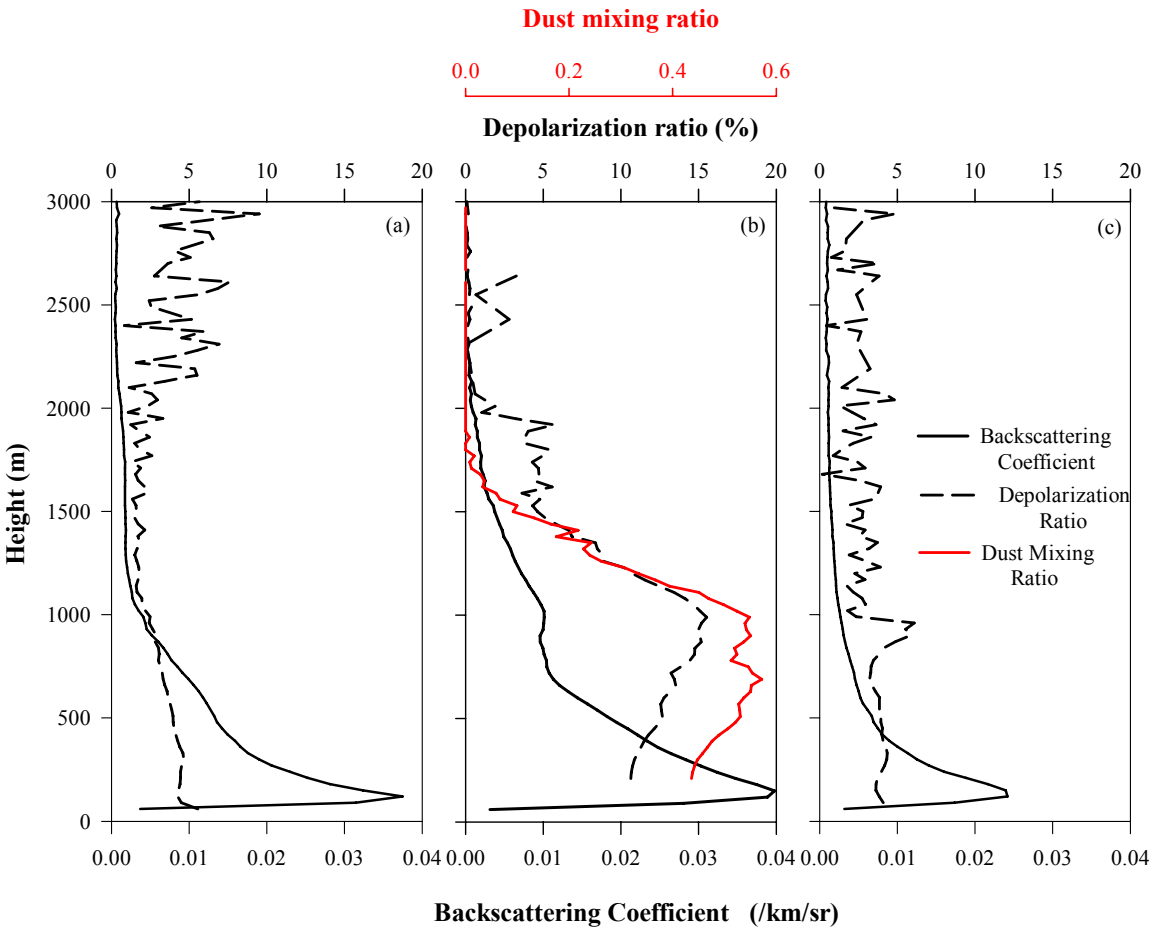

Fig. 9. Vertical profile of backscattering coefficient ($km^{-1}sr^{-1}$) and depolarization ratio (%) during (a) PE1 (1130 - 1500 LST, 6 April), (b) PE2 (0130-0800 LST, 25 April), and (c) PE3 (1130 - 1530 LST, 1 June). The profile of the fraction of dust aerosol extinction to the total aerosol extinction (dust mixing ratio) was calculated and presented during PE2 (Fig. 9b).

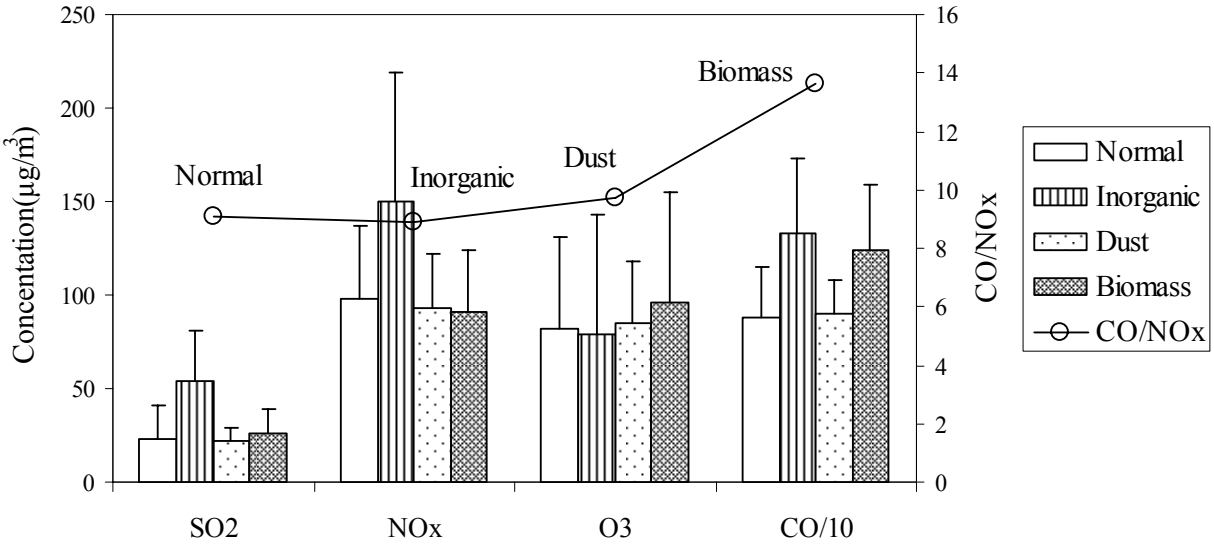

Fig. 10. The average concentrations of SO_2, NOx, O_3 and CO during the normal period, PE1 (inogranic), PE2 (dust), and PE3 (biomass), respectively. The concentrations of CO were divided by 10 for scale visualization, and the ratios of CO/NOx were also calculated and shown in the figure. Error bars represented one standard deviation of the gaseous concentrations during different periods.

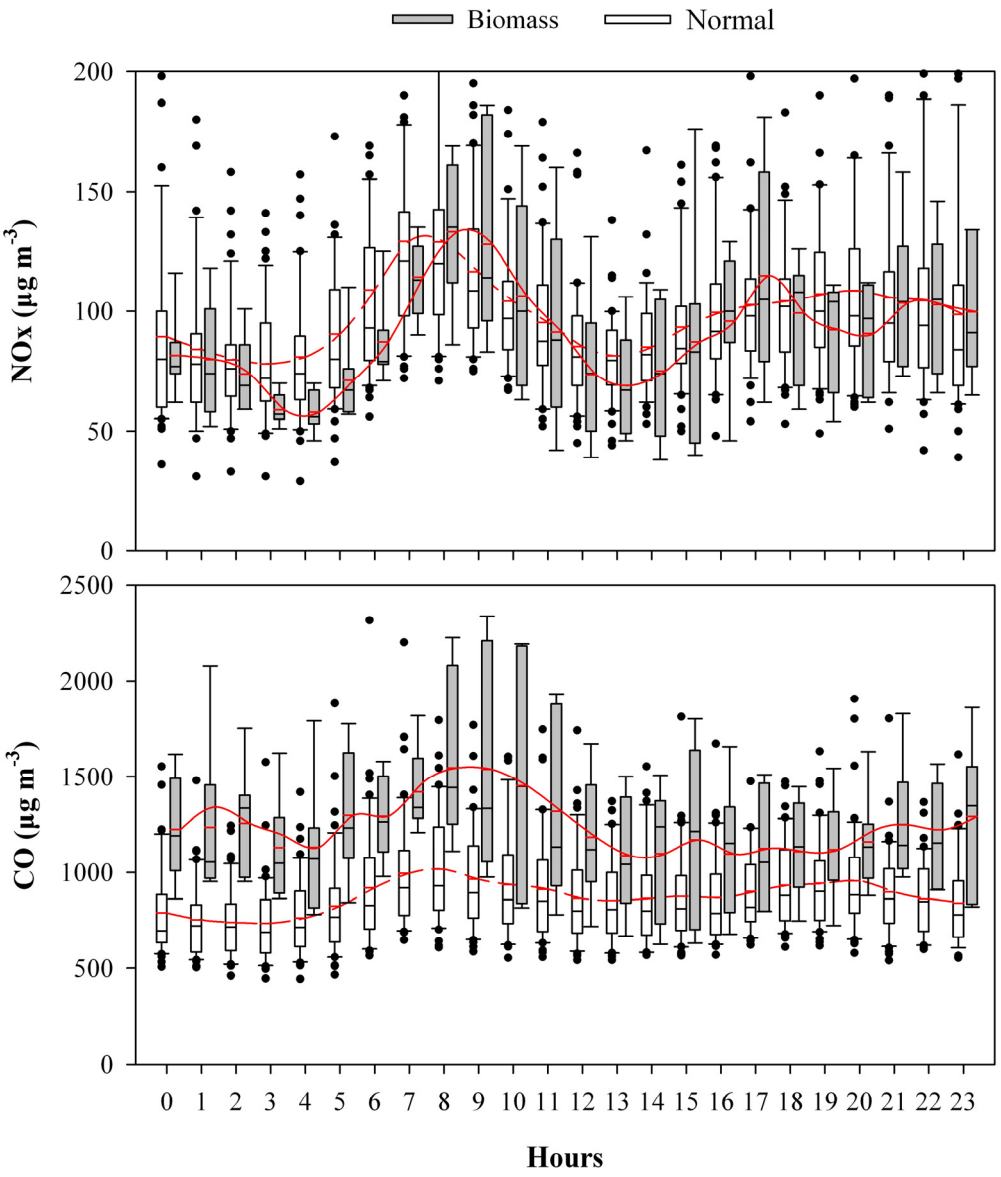

Fig. 11. The diurnal variation of CO and NOx concentrations (µgm^{-3}) during the biomass burning period (gray box) and normal period (white box), respectively. Diurnal mean values are connected by the red spline curves; bottom and top of the boxes represent the 25 and 75% limits, respectively; and bottom and top short lines represent the minimum and maxium values, respectively; Black dots represent the outliers.

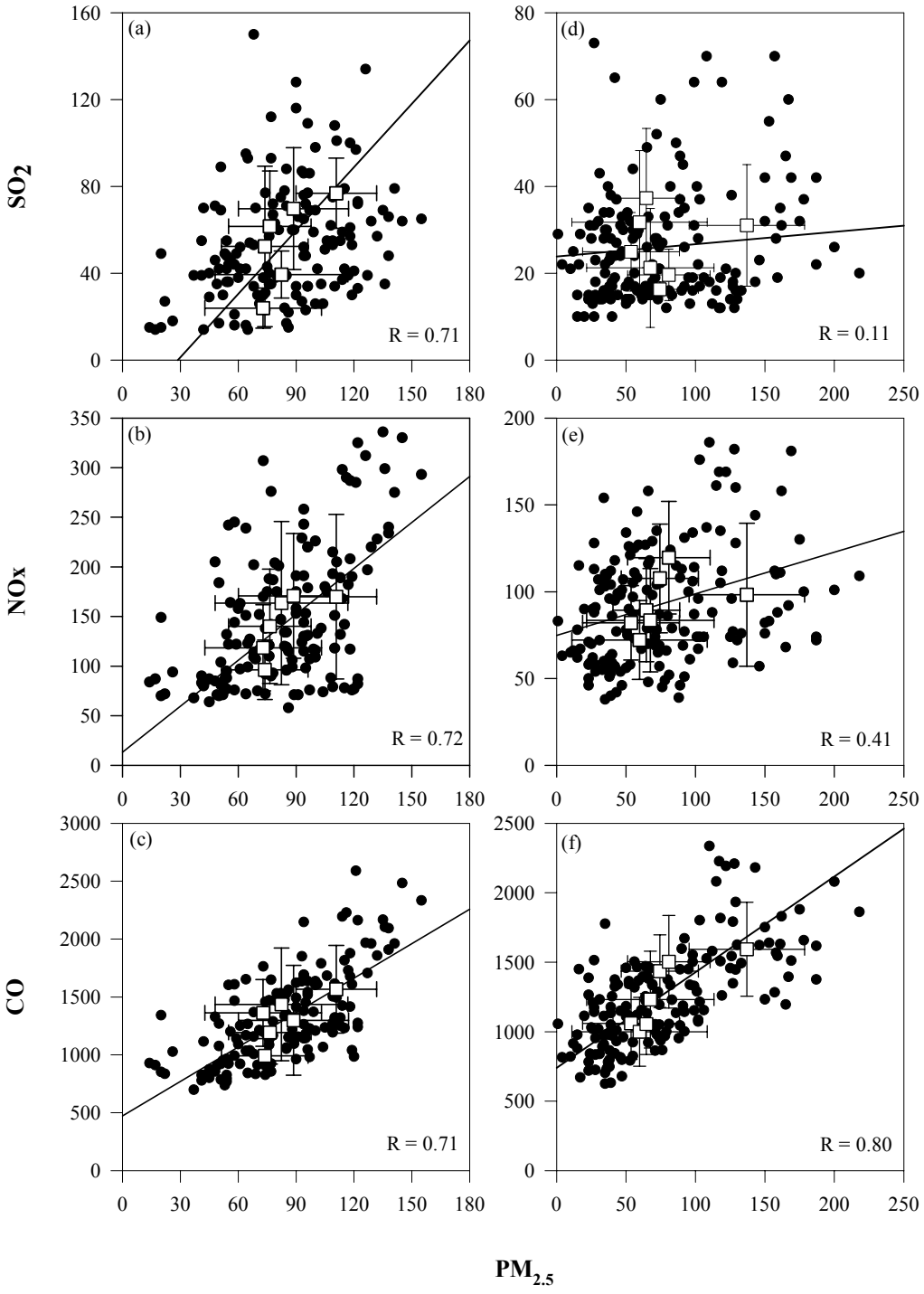

Fig. 12. The linear correlation between gaseous pollutants (SO_2, NOx and CO) and $PM_{2.5}$, with correlation coefficients (R) shown in the figure. (a) - (c) denote PE1 and (d) - (f) denote PE3. The black dots denote the hourly data and the square symbols denote the daily average data, all units are in μgm^{-3}.